

Electrical Capacitance Tomography with a Square Sensor

W Q Yang*

Department of Electrical Engineering and Electronics, Process Tomography Group,
UMIST, P O Box 88, Manchester M60 1QD, UK, email w.yang@umist.ac.uk

S Liu

Institute of Engineering Thermophysics, Chinese Academy of Sciences,
P O Box 2706, Beijing 100080, P R China, email shiliu@hotmail.com

Abstract – In the past, electrical capacitance tomography (ECT) with circular sensors has been extensively investigated. For some industrial applications such as circulating fluidised beds, square sensors are required. Research into this specific area has been carried out at UMIST for the first time. To generate sensitivity maps, the Laplace equation is solved using a finite difference method (FDM). Both the linear back-projection (LBP) and an LBP-based iterative algorithm have been implemented for image reconstruction. Experimental results are very promising.

Keywords: Square sensor, Finite difference method, Iterative algorithm, Capacitance tomography

1. INTRODUCTION

Electrical capacitance tomography (ECT) has an ability to present concentration distributions in two-phase dielectric processes and has been deployed in visualisation of flow patterns, e.g. in circulating fluidised beds [1, 2] and pneumatic conveyors [3, 4]. Over the past few years, image quality and measurement accuracy of ECT have been improved significantly. For example, in a recent experimental investigation the difference between the results obtained from an ECT system and pressure measurements is below 3% under certain conditions [5].

In the past, all ECT systems have been designed for use with circular sensors, normally having 6, 8, 12 up to 16 electrodes. A large number of industrial applications, however, involve square or rectangular geometry, such as most industrial boilers and circulating fluidised beds in thermal engineering. This paper reports, for the first time, the feasibility of ECT with a square sensor.

2. SENSOR STRUCTURE

The sensor is depicted in Fig.1. It consists of 12 measurement electrodes, a plastic frame and a copper shielding. The electrodes of 10 cm in length are mounted onto the outer surface of the plastic frame with 2 mm spacing between

neighbouring electrodes. The cross section of the copper shielding is 80 by 80 mm. The inside dimensions of the plastic frame are 60 by 60 mm. The thickness of the plastic frame is 2 mm.

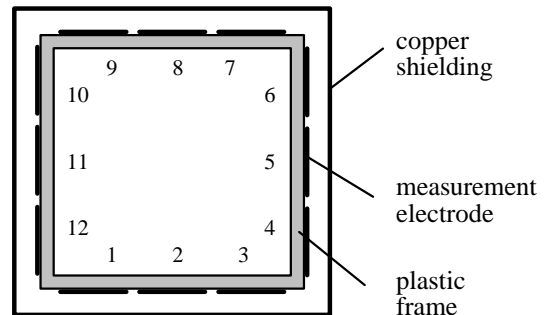


Fig.1 Square sensor

3. GENERATION OF SENSITIVITY MAPS

Sensitivity distributions of a sensor, which are called sensitivity maps, are essential for image reconstruction. In the linear back-projection (LBP) algorithm, for example, an image is obtained by superimposing all sensitivity maps together using capacitance measurements as weighting factors. Although sensitivity maps can be experimentally measured [6], in most cases they are generated from numerical solutions of the Laplace equation. For electrical fields, it is

* W Q Yang is a member of the Virtual Centre for Industrial Process Tomography

$$\frac{\nabla^2 f}{\nabla x^2} + \frac{\nabla^2 f}{\nabla y^2} = 0 \tag{1}$$

where, f is the potential distribution.

Because it is difficult to find analytical solutions of the equation, finite element methods (FEM) are often utilised to solve this problem [7]. Due to the feature of the square sensor, finite difference methods (FDM) seem more suitable than FEM for solving the equation [8, 9]. For the sensor shown in Fig.1, the sensing domain is divided into 160 by 160 square mesh grids and central differencing scheme is used. The procedures are summarised as follows.

One electrode is set a voltage as a source electrode and the remaining electrodes are kept at the earth potential. For a typical internal grid point as shown in Fig.2, its value is determined by

$$f_o = \frac{1}{4} \sum_{i=1}^4 f_i \tag{2}$$

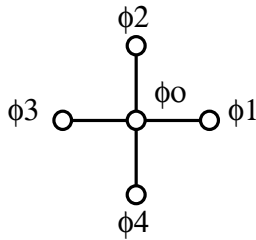


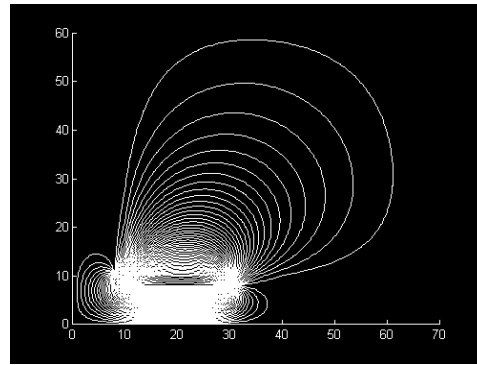
Fig.2 A typical internal grid point

An iterative approach is used to solve the potentials over the whole domain. For the 12-electrode sensor, 12 potential distributions are obtained. Fig.3 shows two typical potential distributions when electrode 1 and electrode 2 are energised, respectively.

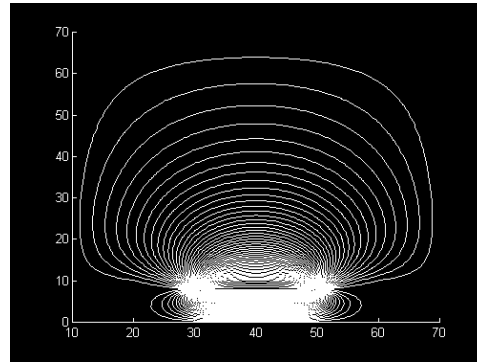
The sensitivity of electrode pair i - j at a spatial location (x, y) is calculated by dot-multiplying the two electric fields.

$$S_{ij}(x, y) = - \int_{p(x,y)} \frac{\vec{E}_i(x, y)}{V_i} \cdot \frac{\vec{E}_j(x, y)}{V_j} dx dy \tag{3}$$

where, $E_i(x, y)$ is the electric field distribution when electrode i is the source electrode with an excitation voltage V_i applied, while other electrodes remain at the earth potential, and $P(x, y)$ is the area of the pixel at (x, y) .



(a) Electrode 1 energised



(b) Electrode 2 energised

Fig.3 Typical potential distributions

Fig.4 illustrates some of the sensitivity maps, showing the higher sensitivity between neighbouring electrodes (e.g. 1 and 2) and the symmetric feature between two opposite electrodes (e.g. 2 and 8).

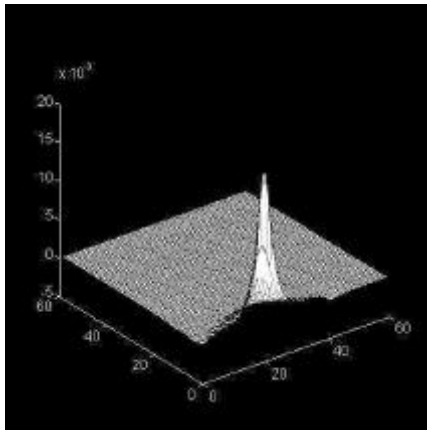
4. IMAGE RECONSTRUCTION

4.1 Linear back-projection

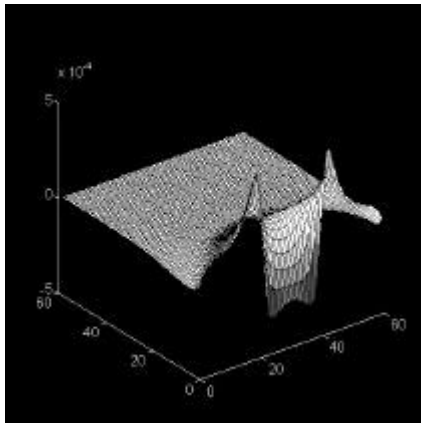
LBP is a simple image reconstruction algorithm and has commonly been used in ECT with circular sensors. For the 12-electrode square sensor, it takes the same format as the circular sensors.

$$G(x, y) = \frac{\sum_{i=1}^{11} \sum_{j=i+1}^{12} C_{ij} S_{ij}(x, y)}{\sum_{i=1}^{11} \sum_{j=i+1}^{12} S_{ij}(x, y)} \tag{4}$$

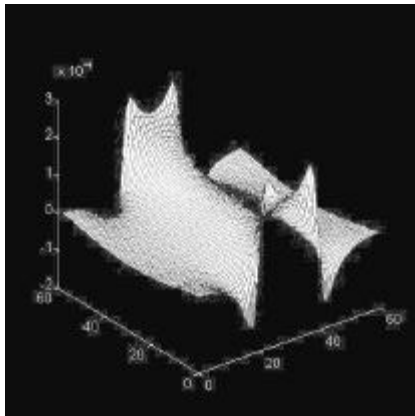
where, $G(x, y)$ is the grey level in a pixel (x, y) , i.e. the reconstructed image, and C_{ij} is the normalised capacitance measurement.



(a) Between electrodes 1 and 2



(b) Between electrodes 1 and 4



(c) Between electrodes 2 and 8

Fig.4 Sensitivity maps calculated using the finite difference method

4.2 Iterative algorithm

To obtain high-quality images, iterative methods have to be used to overcome non-linear problems caused by electric field distortion. An LBP-based iterative algorithm has recently been developed at UMIST and has been used for ECT with circular sensors successfully. Its principle is illustrated in Fig.5 [10]. This algorithm is chosen

for image reconstruction with the square sensor. An initial image \mathbf{G}_k is obtained using the LBP algorithm as shown in equation (4). The estimated capacitance vector \mathbf{D}_k is obtained

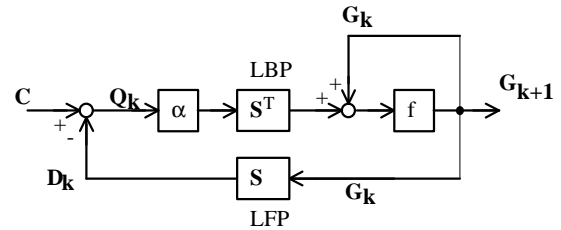


Fig.5 Iterative loop

from the current image by linear forward projection (LFP).

$$D_{k,ij} = \frac{\sum_x \sum_y G_k(x, y) S_{ij}(x, y)}{\sum_x \sum_y S_{ij}(x, y)} \quad (5)$$

The error vector \mathbf{Q}_k is used to reconstruct an error image using the LBP algorithm. The error image is added to the current image and then constrained to get a modified image \mathbf{G}_{k+1} .

$$f(x) = \begin{cases} 0 & (x < 0) \\ x & (0 \leq x \leq 1) \\ 1 & (x > 1) \end{cases} \quad (6)$$

The mathematical expression of the algorithm is as follows.

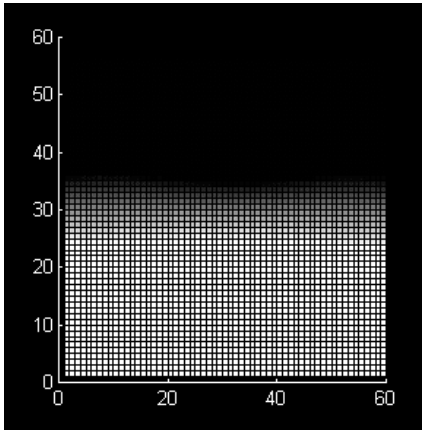
$$\mathbf{G}_{k+1} = f[\mathbf{G}_k + \alpha \mathbf{S}^T (\mathbf{C} - \mathbf{S} \mathbf{G}_k)] \quad (7)$$

5. EXPERIMENTAL EVALUATION

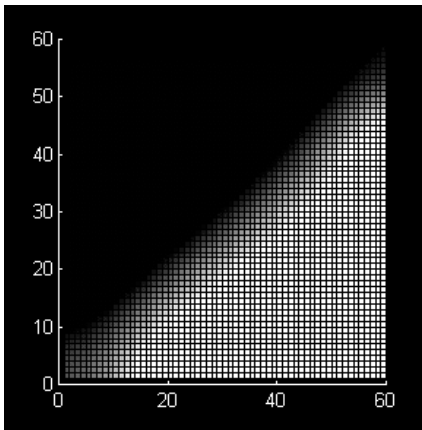
The two algorithms discussed above, LBP and iterative, have been implemented using the MATLAB. Experiments were carried out using an ECT system to evaluate the square sensor performance and to investigate the efficiency of iterative image reconstruction. The sensor was calibrated by air ($\epsilon_r = 1.0$) and plastic pellets ($\epsilon_r = 2.0$) as the lower and higher permittivity materials. It was then tested with plastic pellets and plastic rods ($\epsilon_r = 2.5$). Fig.6 shows some images without iterations: (1) horizontally half-filled with plastic pellets, (2) diagonally half-filled with plastic pellets, and (3) a round plastic rod in the centre.

Fig.7 shows another set of images for three circular rods placed in the imaging area, one without iterations and another with 10 iterations. Obviously the image produced by LBP only shows a blurred area, but not three objects. In contrast, the image produced by the iterative

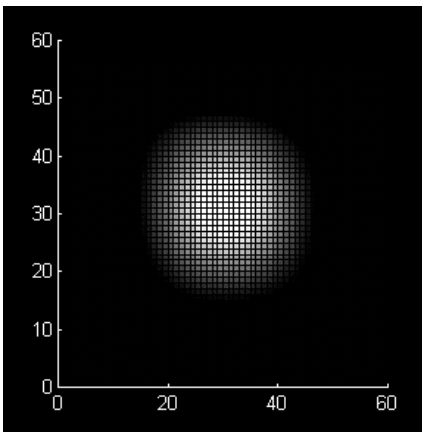
algorithm shows three objects clearly. This indicates significant improvement by iterations.



(a) Horizontally half-filled with plastic pellets

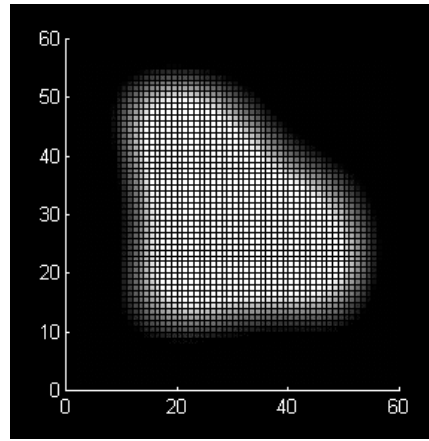


(b) Diagonally half-filled with plastic pellets

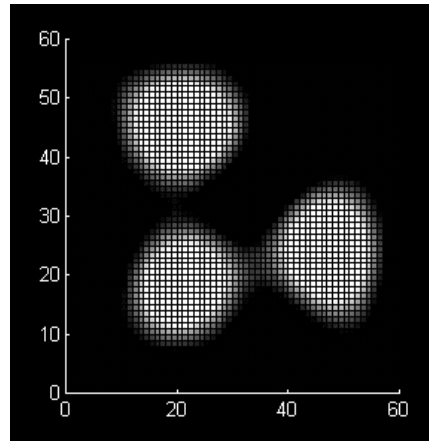


(c) A round plastic rod in the centre

Fig.6 Reconstructed images without iteration



(a) Before iterations



(b) After iterations

Fig.7 Reconstructed images with three plastic rods

6. CONCLUSION AND DISCUSSION

Some industrial applications require square sensors, such as circulating fluidised beds. The sensitivity distributions of a square sensor can be calculated using FDM which is easier to be implemented than FEM. Once sensitivity maps have been obtained, images can be reconstructed using MATLAB with easy. The iterative algorithm based on LFP and LBP has demonstrated very good performance.

Many experimental results show that the quality of image from the square sensor is better than that from a circular sensor. As can be seen in Fig.4, the sensitivity distributions of the square sensor are more uniform between two sensing electrodes, than those of a circular sensor. It is believed that the sensitivity in the centre (the weakest area) of a square sensor is higher than that of a circular sensor, and hence a square sensor can provide better image resolution than a circular sensor.

For a square sensor to be used in a real-size industrial fluidised bed, it is necessary to cope with a large scale, say 2 by 2 meters. A difficulty with this is that the current ECT system would not

be appropriate for so long shielding cables. This problem will be addressed in the near future.

ACKNOWLEDGEMENTS

The authors would like to thank Dr. M.Wang and Prof. H.McCann of UMIST, Mr. M.Byars of Process Tomography Ltd, Dr. D.M.Spink of University of Leeds and Prof. H.X.Wang of Tianjin University (on visiting to UMIST) for their help in this work.

REFERENCES

- [1] S.Wang, T.Dyakowski. and M.S.Beck, "Application of electrical capacitance tomography to measure gas-solid motion in fluidized bed", in Heat-transfer, AICHE symposium series, Houston, 1996, pp 155-160
- [2] J.S.Halow, "Capacitance imaging of fluidized beds", in Process Tomography -- Principles, Techniques and Applications, edited by R.A.Williams and M.S.Beck, Butterworth Heinemann, 1995, pp 447-486
- [3] S.L.McKee, T.Dyakowski, R.A.Williams, T.A.Bell and T.Allen, "Solids flow imaging and attrition studies in a pneumatic conveyor", Powder Technology, 1995, 82, pp 105-113
- [4] S.P.Luke and R.A.Williams, "Industrial applications of electrical tomography to solids conveying", Measurement + Control, 1997, 30, pp 201-205
- [5] S.Liu, S.Wang, D.Mason, T.Dyakowski and D.Geldart, "Measurement of solids concentration in gas-solid flows using capacitance tomography and pressure sensors", in Sensors and their Applications VIII, Proc. of the 8th Conf. on Sensors and their Applications, Glasgow, September 1997, edited by A.T.Augousti and N.M.White, Institute of Physics Publishing, Bristol and Philadelphia, pp 101-105.
- [6] W.Q.Yang, and W.F.Conway, "Measurement of sensitivity distributions of capacitance tomography sensors", Rev. Sci. Instrum., 1998, 69, pp 233-236.
- [7] D.M.Spink, "Direct finite element solution for the capacitance, conductance or inductance, and force in linear electrostatic and magnetostatic problems", COMPEL, 1996, 15, pp 70-84
- [8] J.D.Anderson, Computational fluid dynamics -- The basics with applications, McGraw-Hill Inc., Singapore, 1995
- [9] C.H.Qiu, Electrical resistance tomography for imaging sub-seabed sediment porosity, MSc Thesis, UMIST, 1995
- [10] W.Q.Yang, D.M.Spink, T.A.York and H.McCann, "An image reconstruction algorithm based on Lanweber iteration method for capacitance tomography", (submitted to IEEE Trans. Image Processing)